The strength of the radial-breathing mode in single-walled carbon nanotubes

M. Machón[*], S. Reich[†], J. Maultzsch[*], P. Ordejón[**] and C. Thomsen[*]

[*]Institut für Festkörperphysik, Technische Universität Berlin, Hardenbergstr. 36, 10623 Berlin, Germany
[†]University of Cambridge, Department of Engineering, Trumpington Street, Cambridge CB2 1PZ, United Kingdom
[**]Institut de Ciència de Materials de Barcelona (CSIC), Campus de la U.A.B. E-08193 Bellaterra, Barcelona, Spain

Abstract. We present calculations of the absolute Raman cross section of the radial breathing mode (RBM) of single-walled carbon nanotubes. We included all matrix elements explicitly as obtained from first principles calculations. Our results show a systematic dependence on diameter and chiral angle as well as on $\nu = (n_1 - n_2) \bmod 3$, which we explain with the help of a zone folding model. Thus, the comparison of relative Raman intensities can serve as an independent check for chirality assignments. The dependencies come mainly from the electron-phonon matrix elements $\mathcal{M}_{e-ph}$, which have to be taken into account when dealing with absolute Raman intensities. We compare our calculations to measurements of the absolute Raman cross section of individual nanotubes and find an agreement to within one order of magnitude. The obtained intensities are consistent with the fact that the Raman signal of a single nanotube can be detected experimentally.

One of the most interesting characteristics of single-walled nanotubes is the dependence of their physical properties on the particular geometry, defined through the diameter and chirality. Assigning chiral indices to carbon nanotubes is thus essential for research and application, but a reliable technique is not available yet. Interesting proposals were based on luminescence or Raman measurements [1, 2, 3, 4]. In particular, the frequency of the radial-breathing mode (RBM) with its roughly linear dependence on the nanotube diameter [5, 6] is widely used to determine the diameters present in samples. Here, we show how the Raman intensities of the RBM yield information about the chirality as well as the diameter, which can be used in an (n_1, n_2)-assignment.

The first-order Raman scattering cross section per unit length and solid angle can be expressed as

$$\frac{dS}{d\Omega} = \frac{\omega_l \omega_s^3 \, n_l n_s^3 V_c N}{(2\pi)^2 c^4 (\hbar \omega_l)^2} \left[n_{be}(\omega_{ph}) + 1 \right] \left| \int \frac{\rho(\hbar\omega) \mathcal{M}_{e-r} \, \mathcal{M}_{e-ph} \, \mathcal{M}_{e-r} \hbar}{(E_l - \hbar\omega - i\gamma)(E_l - \hbar\omega_{ph} - \hbar\omega - i\gamma)} \, d\omega \right|^2 .$$

A lot of work has been devoted to the resonance conditions expressed by the denominator of this equation [7]. In this work we rather concentrate on the numerator needed to determine the resonance intensity. In particular, we determined the electron-phonon coupling matrix elements using the *ab initio* package SIESTA [8, 9]. Using the calculated matrix elements we find absolute Raman intensities for single-walled carbon nanotubes.
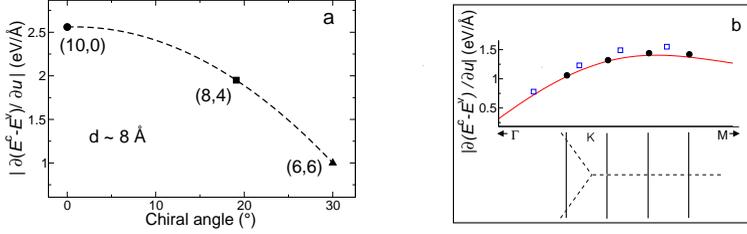
FIGURE 1. **a)** $|\partial(E^c - E^v)/\partial u|$ as function of the chiral angle for three nanotubes with diameter ≈ 8 Å. The dotted line is just a guide for the eye. **b)** $|\partial(E^c - E^v)/\partial u|$ for the (19,0) (dots) and (17,0) (squares) nanotubes mapped onto the Γ-K-M direction of the Brillouin zone of graphene. The gray line corresponds to a calculation for graphene in which we stretched the direction corresponding to the circumference of a zig-zag nanotube in order to simulate the RBM of a (19,0) nanotube. A part of the reciprocal space of graphene is shown below (dashed lines) together with some of the lines of allowed k-points which form the Brillouin zone of a (19,0) nanotube. The data points for the (19,0) nanotube are placed above the k-point lines they correspond to.

Calculations were performed within the local density approximation [10]. We replaced the core electrons by non-local norm-conserving pseudopotentials [11]. A grid cutoff of ≈ 270 Ry was used for real space integrations. A double-ζ, singly polarized basis set of localized atomic orbitals was used for the valence electrons, with cutoff radii of 5.12 a.u. for the s and 6.25 a.u. for the p and d orbitals [12]. 16 k points in the k_z direction were included for metallic nanotubes and 3 k points for semiconducting tubes. The matrix elements $\mathscr{M}_{e-ph}$ were calculated using the phonons obtained with a finite differences approach.

The absolute value of the matrix element tends to be smaller for bigger nanotubes [up to 0.017 eV for the (19,0) nanotube and 0.031 eV for the (10,0) nanotube]. This is expected since the RBM becomes a pure translation in the infinite-diameter limit, which cannot interact with the electronic system.

For totally symmetric Γ-point vibrations the electron-phonon matrix elements can be calculated by [13]:

$$\mathscr{M}_{e-ph} = C \sum_a \varepsilon_a^i \frac{\partial [E^c(\boldsymbol{k}) - E^v(\boldsymbol{k})]}{\partial \boldsymbol{u}_a}, \tag{1}$$

where $\boldsymbol{k}$ denotes the wave vector of the electronic state, c (v) denotes the conduction (valence) band which participates in a particular optical transition, i indexes the phonon with polarization vector ε_a^i normalized as $\sum_a \varepsilon_a^i \varepsilon_a^j = \delta_{ij}$, $\boldsymbol{u}_a$ is the atomic displacement, and C a normalization factor. In Fig. 1a we show an example of the chirality dependence of the electron-phonon coupling. The values of $|\partial(E^c - E^v)/\partial u|$ for the first transition of three nanotubes with diameter ≈ 8 Å are shown. As can be seen, the electron-phonon coupling for these three nanotubes decreases for increasing chiral angle. This invalidates the widespread assumption that the electron-coupling is constant for all nanotubes and means that it has to be taken into account when dealing with Raman intensities.

We find another systematic dependence of our data on the chiral indices: namely that on the value of $\nu = \pm 1$. If we denote by $\mathscr{M}_{1,2}$ the matrix elements corresponding to the
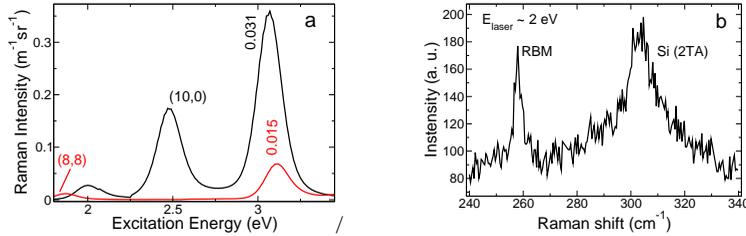
FIGURE 2. **a)** Raman resonance profile for the (10,0) and (8,8) nanotubes calculated including all matrix elements explicitly. Close to the ≈ 3 eV resonances, the corresponding electron-phonon matrix elements are written, in eV. **b)** measurement of the RBM of an isolated SWNT and the second order 2TA phonon of Si coming from the substrate. [15]

first and second optical transition, respectively, we obtain $|\mathcal{M}_1/\mathcal{M}_2| < 1$ for $\nu = -1$, but $|\mathcal{M}_1/\mathcal{M}_2| > 1$ for $\nu = +1$.

In Fig. 1b we show $|\partial(E^c - E^v)/\partial u|$ for a nanotube of each of these two families. The gray line shows a calculation in which we stretched a sheet of graphite in the direction corresponding to the circumference of zigzag nanotubes. This corresponds to the RBM of a (19,0) nanotube and yields an excellent agreement with the full calculation as can be seen in the figure. The *x*-axis corresponds to the Γ-*K*-*M* direction in the reciprocal space of graphene. This space is shown by the dashed lines in the lower half of the figure, together with some of the lines of allowed *k*-points which form the Brillouin zone of the (19,0) nanotube (solid lines). Each of these lines gives rise to an optical transition, to which an $\mathcal{M}_{e-ph}$ corresponds, [for the (19,0) nanotube each data point is placed above the *k*-point line it corresponds to]. Since the graphene bands are linear close to the *K*-point, the energies of the optical transitions are higher the closer from *K* they originate. Therefore, for the (19,0) nanotube the lowest transition E_{11} comes from the right from the *K*-point, E_{22} from the left, etc [14]. As can be seen in the figure, the electron-phonon coupling is lower on the left of the *K* point than on its right, thus, for the (19,0) nanotube $|\mathcal{M}_1/\mathcal{M}_2| > 1$. This applies for all nanotubes of the +1 family. For the (17,0) nanotube, on the other hand, the first transition is on the left, the second on the right, etc, yielding $|\mathcal{M}_1/\mathcal{M}_2| < 1$. Analogously for all nanotubes of the −1 family. We propose to measure and compare relative Raman intensities of consecutive optical transitions to discriminate this two families of nanotubes for which other physical properties like transition energies or RBM frequencies are too similar to allow the full characterisation.

We now calculate the absolute Raman cross section including explicitly all matrix elements as calculated *ab initio*. In Fig. 2 we show calculated Raman profiles for the (10,0) and (8,8) nanotubes. The resonance intensity at 3 eV differs by a factor of ≈ 4, which comes mainly from $|\mathcal{M}_{e-ph}|^2$ as can be seen from the $\mathcal{M}_{e-ph}$ values (in eV) indicated close to the peaks. We obtained an experimental value of the absolute Raman intensity of carbon nanotubes by comparing a measured RBM peak with the Si (2TA) peak at $300\,\mathrm{cm}^{-1}$ [15] (see Fig. 2b), yielding $dS_{RBM}/d\Omega \approx dS_{Si,2TA}/d\Omega \times 1.2\,10^6 = 1.1\ \mathrm{m}^{-1}\mathrm{sr}^{-1}$. In Fig. (2), the intensities at 2 eV are $\approx 0.01\text{-}0.03\,\mathrm{m}^{-1}\mathrm{sr}^{-1}$, two orders of magnitude lower than the experiment. In view of the difficulties of this type of

measurements and calculations (the errors can amount up to one order of magnitude), the agreement is quite good. Both our calculated and measured values are very high if compared with measured Raman intensities for other materials (for instance the first order mode of Si: $dS/d\Omega = 1.68\,10^{-5}$ m^{-1}sr^{-1}) [16]. Our calculations thus explain why Raman scattering of a single, isolated nanotube can be observed experimentally. [15, 17]

We performed analogous calculations of the matrix elements $\mathscr{M}_{\text{e-ph}}$ for the high-energy mode. Comparing the matrix elements for the two phonons, we obtain $\mathscr{M}_{\text{e-ph}}^{\text{HEM}}/\mathscr{M}_{\text{e-ph}}^{\text{RBM}} \approx 4-6$ depending on the particular nanotube and electronic transition. The matrix elements for the HEM show a similar dependence on chirality and $(n_1 - n_2)\,\mathrm{mod}\,3$.

In conclusion, we studied the effect of the electron-phonon coupling of carbon nanotubes on the Raman intensity of the radial breathing mode. Our study shows systematic dependences on diameter and chirality which can be used in (n_1, n_2)-assignments of nanotube samples. We calculated absolute Raman intensities of the radial breathing mode and compared them to experimental results. The extremely large experimental and theoretical cross section explains why an individual nanotube can be observed by Raman scattering.

ACKNOWLEDGMENTS

REFERENCES

1. Bachilo, S. M., Strano, M. S., Kittrel, C., Hauge, R. H., Smalley, R. E. and Weisman, R. B., *science*, **298**, 2361 (2002).
2. Strano, M. S. *et al.*, *Nano Letters*, **3**, 1091 (2003).
3. Kramberger, C. *et al.*., *Phys. Rev. B*, **68**, 235404 (2003).
4. Telg, H., Maultzsch, J., Reich, S., Henrich, F. and Thomsen, C. (submitted).
5. Rao, A. M. *et al.*, *Science*, **275**, 187 (1997).
6. Kürti, J., Kresse, G. and Kuzmany, H., *Phys. Rev. B*, **58**, 8869 (1998).
7. Thomsen, C. and Reich, S., *Phys. Rev. Lett.*, **85**, 5214 (2000).
8. Ordejón, P., Artacho, E. and Soler, J. M., *Phys. Rev. B*, **53**, R10 441 (1996).
9. Soler, J. M. *et al.*, *J. Phys. Condens. Mat.*, **14**, 2745 (2002).
10. Perdew, J. P. and Zunger, A., *Phys. Rev. B*, **23**, 5048 (1981).
11. Troullier, N. and Martins, J., *Phys. Rev. B*, **43**, 1993 (1991).
12. Junquera, J., Paz, O., Sánchez-Portal, D. and Artacho, E., *Phys. Rev. B*, **64**, 235111 (2001).
13. Khan, F. and Allen, P., *Phys. Rev. B*, **29**, 3341 (1984).
14. Reich, S., , Thomsen, C. and Ordejón, P., *Phys. Rev. B*, **65**, 155411 (2002).
15. Maultzsch, J., Reich, S., Schlecht, U. and Thomsen, C., *Phys. Rev. Lett.*, **91**, 087402 (2003).
16. Cardona, M., "Resonance Phenomena," in *Light Scattering in Solids II*, edited by M. Cardona and G. Güntherodt, Springer, Berlin, 1982, vol. 50 of *Topics in Applied Physics*, p. 19.
17. Jorio, A. *et al.*, *Phys. Rev. B*, **63**, 245416 (2001).